Blind Source Separation of Instantaneous Mixture of Delayed Sources Using High-Order Taylor Approximation

Wei Zhao, Zhigang Yuan, Yuehong Shen, Yufan Cao, Yimin Wei, Pengcheng Xu, and Wei Jian

This paper deals with the problem of blind source separation (BSS), where observed signals are a mixture of delayed sources. In reference to a previous work, when the delay time is small such that the first-order Taylor approximation holds, delayed observations are transformed into an instantaneous mixture of original sources and their derivatives, for which an extended second-order blind identification (SOBI) approach is used to recover sources. Inspired by the results of this previous work, we propose to generalize its first-order Taylor approximation to suit higher-order approximations in the case of a large delay time based on a similar version of its extended SOBI. Compared to SOBI and its extended version for a first-order Taylor approximation, our method is more efficient in terms of separation quality when the delay time is large. Simulation results verify the performance of our approach under different time delays and signal-to-noise ratio conditions, respectively.

Keywords: Blind source separation, second-order blind identification, first-order Taylor approximation, high-order Taylor approximation, signal-to-noise ratio.

Manuscript received Apr. 29, 2014; revised Oct. 14, 2014; accepted Apr. 15, 2015.

This work was supported by the National Natural Science Foundation of China under Grant No. 61172061 and 61201242, and NSF of Jiangsu Province of China under Grant No. BK2012057.

Wei Zhao (gmajyie@126.com), Zhigang Yuan (corresponding author, yzhigang_cn@163.com), Yuehong Shen (chunfeng22259@126.com), Yufan Cao (13515110797@163.com), Yimin Wei (weiym73@163.com), Pengcheng Xu (b71087@126.com), and Wei Jian (jw_jian@163.com) are with Wireless Communications Center, the College of Communications Engineering, PLA University of Science and Technology, Nanjing, China.

I. Introduction

Blind source separation (BSS) has been applied in a variety of fields in recent decades, such as telecommunication, speech processing, array processing, passive sonar, seismic exploration, and so on [1]. In the case of a linear multiple-input and multiple-output instantaneous system, BSS corresponds to independent component analysis (ICA), which is now a widely recognized concept [2].

However, ICA is not suitable for practical application, since observed signals are not only linear and instantaneous but are a convolutive mixture of sources [3]; for example, wireless communication signals received by antennas are usually composed of delay and reflected echoes of transmitted sources. The propagation time of each speaker's voice to different microphones at a cocktail party differs, obviously. Similarly, myoelectric signals recorded in multiple locations over the surface of a person's skin are not only attenuated by a volume conductor but also represent delayed versions of source signals because of the propagation of the intracellular potentials along the person's muscle fibers. In fact, the observed signals of the sources in these practical applications can be modeled, in general, as a convolutive mixture.

In this paper, we consider a particular case of the general convolutive mixture problem: instantaneous mixtures of delayed sources, which can be seen as a special case of the convolution model — a very common model in BSS.

The observed signals $\mathbf{x}(t)=[x_1(t), x_2(t), \ldots, x_M(t)]^{\mathrm{T}}$ composed of delayed source signals can be modeled as

$$\mathbf{x}(t)=\mathbf{A}\mathbf{s}(t-\tau)+\mathbf{p}(t), \tag{1}$$

where $\mathbf{A}$ is an $M \times N$ mixing matrix, the delayed sources $\mathbf{s}(t-\tau)=[s_1(t-\tau_1), s_2(t-\tau_2), \ldots, s_N(t-\tau_N)]^{\mathrm{T}}$, where $\tau_1, \ldots, \tau_N$ are the time delays, and the receiver noise vector $\mathbf{p}(t)=[p_1(t), p_2(t), \ldots, p_M(t)]^{\mathrm{T}}$. Each component of a mixed-signals vector can be formulated as

$$x_i(t)=\sum_{j=1}^{N} a_{ij} s_j(t-t_{ij})+p_i(t), \quad i=1,2, \ldots, M, \tag{2}$$

where t_{ij} is the delayed time of sources, N is the number of source signals, M is the number of mixed signals, and a_{ij} is an element of $\mathbf{A}$. Equation (2) is the "instantaneous mixture of delayed sources" model considered in this paper. Note that the value of the time delay t_{ij} will, in general, differ from source to source. In other words, the instantaneous mixture of delayed sources model in this paper includes the case where the time delay t_{ij} is the same for any two or more given sources.

As far as we know, there are a few works [4]–[7] concerning BSS of delayed sources. For example, stochastic time-frequency analysis algorithms have been proposed in [6]–[7], and truncated Taylor series expansion algorithms have been explored in [4]–[6]. As shown in [6], if the delay is small, as in

$$t_{ij} \ll t_{\mathrm{d}}=\frac{1}{\sqrt{2\pi} f_{\max}}, \tag{3}$$

where $f_{\max}$ is the maximum frequency of sources, then the delayed observations can be transformed into an instantaneous mixture of original sources and their derivatives by using a first-order Taylor approximation. A first-order Taylor approximation of (2) can be formulated by

$$x_i(t)=\sum_{j=1}^{N} a_{ij} s_j(t)-\sum_{j=1}^{N} a_{ij} t_{ij} s_j^{(1)}(t)+p_i(t), \quad i=1,2,\ldots,M, \tag{4}$$

where $s_j(t-t_{ij}) \approx s_j(t)-t_{ij} s_j^{(1)}(t)$ is applied in (2) and $s_j^{(1)}(t)$ is the first-order derivative of $s_j(t)$. The sources are recovered by extending the second-order blind identification (SOBI) approach of [8] and [9], which exploits the spatial covariance matrix or spatial time-frequency representation of whitened observations to recover sources through identification of a rotation matrix.

Inspired by [6], we propose to deal with the blind separation of delayed sources in the case of large delay using high-order Taylor approximations based on a similar extended version of the SOBI approach found in [6], [8], and [9]. In the noiseless case, our proposed method outperforms other corresponding approaches in terms of separation quality when the delay is large. When noise is introduced, our method provides approximately identical performance to the aforementioned corresponding approaches in the case of small delay but performs much better in the case of large delay, which validates the robustness of our method. A performance comparison and analysis are investigated through simulations.

This paper is organized as follows. Section II introduces our proposed high-order Taylor approximation procedure, in which an extended version of a SOBI approach including whitening and rotation is presented. The simulation results and analysis are performed in Section III. Section IV concludes this paper.

II. High-Order Taylor Approximation

Similar to the first-order approximation in (4) in [6], a high-order Taylor expansion is denoted by

$$\begin{aligned} x_i(t)=&\sum_{j=1}^{N} a_{ij} s_j(t)-\sum_{j=1}^{N} a_{ij} t_{ij} s_j^{(1)}(t)+\sum_{j=1}^{N} a_{ij} \frac{t_{ij}^{\,2}}{2} s_j^{(2)}(t) \\ &-\sum_{j=1}^{N} a_{ij} \frac{t_{ij}^{\,3}}{6} s_j^{(3)}(t)+\cdots+\sum_{j=1}^{N} a_{ij} \frac{t_{ij}^{\,n}}{n!} s_j^{(n)}(t)+p_i(t), \\ & i=1,2, \ldots, M, \end{aligned} \tag{5}$$

where $s_j^{(n)}(t)$ is the nth-order derivative of $s_j(t)$. Then, the delayed source vector, $\mathbf{s}(t-\tau)$, can be extended as $\overline{\mathbf{s}(t)}=[s_1(t), \ldots, s_N(t), s_1^{(1)}(t), \ldots, s_N^{(1)}(t), \ldots, s_1^{(n)}(t), \ldots, s_N^{(n)}(t)]^{\mathrm{T}}$, and mixing matrix $\mathbf{A}$ can be extended to $\overline{\mathbf{A}}$ as

$$\overline{\mathbf{A}}=\left[\mathbf{A}^0 \quad \mathbf{A}^1 \quad \mathbf{A}^2 \quad \cdots \quad \mathbf{A}^n\right], \tag{6}$$

where

$$\mathbf{A}^n=\frac{(-1)^n}{n!}\begin{pmatrix} a_{11}t_{11}^n & a_{12}t_{12}^n & \ldots & a_{1N}t_{1N}^n \\ a_{21}t_{21}^n & a_{22}t_{22}^n & \ldots & a_{2N}t_{2N}^n \\ \vdots & \vdots & \ddots & \vdots \\ a_{M1}t_{M1}^n & a_{M2}t_{M2}^n & \ldots & a_{MN}t_{MN}^n \end{pmatrix}. \tag{7}$$

Finally, we can reformulate the time-delayed BSS model as an "instantaneous mixture of original sources and their nth-order derivatives" model; that is, $\mathbf{x}(t)=\overline{\mathbf{A}}\overline{\mathbf{s}(t)}+\overline{\mathbf{p}(t)}$, in which $\overline{\mathbf{p}(t)}=[\mathbf{p}(t), \mathbf{p}(t), \ldots, \mathbf{p}(t)]$. Note that the number of sources increases to $(n+1)N$ equivalently; so, we assume that $M \geq (n+1)N$ to ensure the separability of algorithms in this paper.

To recover sources successfully by using the SOBI approach, we make the following two assumptions:

- The sources are mutually uncorrelated; have zero-mean and unit variance; and are of different spectra. More precisely, the source vector is spatially white and normalized in power; that is,

$$\mathrm{E}\{s_i s_j\}=0, \quad i \neq j, \ \mathrm{E}\{s_i\}=0, \ \mathrm{E}\{s_i^{\,2}\}=1.$$

- The noise vector is mutually uncorrelated, and the components of the source vector and elements of the noise vector are also mutually uncorrelated; that is,

$$\mathrm{E}\{p_i p_j\} = 0, \quad i \neq j, \quad \mathrm{E}\{p_i s_j\} = 0, \quad i, j = 1, \ldots, N,$$

where $\mathrm{E}\{\bullet\}$ denotes the expectation value.

As previous researches have indicated, [6], [8], and [9], this kind of BSS problem can be solved in two steps: (1) whitening and (2) rotation. Whitening consists of deriving a matrix that whitens observations at zero time lag (it is equivalent to principal component extraction, but with normalization of the variances of components); rotation allows for recovery of sources from the whitened observation.

1. Whitening

The covariance matrix of $\overline{\mathbf{s}(t)}$ can be formulated as

$$\mathrm{R}_{\bar{\mathbf{s}}}(\tau) = \begin{bmatrix} \mathrm{R}_{\boldsymbol{ss}}(\tau) & \mathrm{R}_{\boldsymbol{ss}^{(1)}}(\tau) & \ldots & \mathrm{R}_{\boldsymbol{ss}^{(n)}}(\tau) \\ \mathrm{R}_{\boldsymbol{s}^{(1)}\boldsymbol{s}}(\tau) & \mathrm{R}_{\boldsymbol{s}^{(1)}\boldsymbol{s}^{(1)}}(\tau) & \ldots & \mathrm{R}_{\boldsymbol{s}^{(1)}\boldsymbol{s}^{(n)}}(\tau) \\ \vdots & \vdots & \ddots & \vdots \\ \mathrm{R}_{\boldsymbol{s}^{(n)}\boldsymbol{s}}(\tau) & \mathrm{R}_{\boldsymbol{s}^{(n)}\boldsymbol{s}^{(1)}}(\tau) & \ldots & \mathrm{R}_{\boldsymbol{s}^{(n)}\boldsymbol{s}^{(n)}}(\tau) \end{bmatrix}, \tag{8}$$

where

$$\begin{aligned} &\mathrm{R}_{\boldsymbol{ss}}(\tau) = \mathrm{Diag}[\mathrm{R}_{s_1 s_1}(\tau), \mathrm{R}_{s_2 s_2}(\tau), \ldots, \mathrm{R}_{s_N s_N}(\tau)], \\ &\mathrm{R}_{\boldsymbol{ss}^{(1)}}(\tau) = \mathrm{Diag}[\mathrm{R}_{s_1 s_1^{(1)}}(\tau), \mathrm{R}_{s_2 s_2^{(1)}}(\tau), \ldots, \mathrm{R}_{s_N s_N^{(1)}}(\tau)], \\ &\mathrm{R}_{\boldsymbol{s}^{(1)}\boldsymbol{s}}(\tau) = \mathrm{Diag}[\mathrm{R}_{s_1^{(1)} s_1}(\tau), \mathrm{R}_{s_2^{(1)} s_2}(\tau), \ldots, \mathrm{R}_{s_N^{(1)} s_N}(\tau)], \\ &\mathrm{R}_{\boldsymbol{ss}^{(2)}}(\tau) = \mathrm{Diag}[\mathrm{R}_{s_1 s_1^{(2)}}(\tau), \mathrm{R}_{s_2 s_2^{(2)}}(\tau), \ldots, \mathrm{R}_{s_N s_N^{(2)}}(\tau)], \\ &\mathrm{R}_{\boldsymbol{s}^{(2)}\boldsymbol{s}}(\tau) = \mathrm{Diag}[\mathrm{R}_{s_1^{(2)} s_1}(\tau), \mathrm{R}_{s_2^{(2)} s_2}(\tau), \ldots, \mathrm{R}_{s_N^{(2)} s_N}(\tau)], \\ &\quad\vdots \qquad\qquad \vdots \\ &\mathrm{R}_{\boldsymbol{s}^{(n)}\boldsymbol{s}^{(n)}}(\tau) = \mathrm{Diag}[\mathrm{R}_{s_1^{(n)} s_1^{(n)}}(\tau), \mathrm{R}_{s_2^{(n)} s_2^{(n)}}(\tau), \ldots, \mathrm{R}_{s_N^{(n)} s_N^{(n)}}(\tau)]. \end{aligned} \tag{9}$$

As shown in [10], we can draw the following conclusions:

$$\begin{aligned} &\mathrm{R}_{s_i s_i^{(m)}}(\tau) = \mathrm{R}_{s_i s_i}^{(m)}(\tau), \quad m = 1, 2, 3, \ldots, n, \\ &\mathrm{R}_{s_i^{(m)} s_i}(\tau) = -\mathrm{R}_{s_i s_i}^{(m)}(\tau), \quad m = 1, 3, \ldots, 2n-1, \\ &\mathrm{R}_{s_i^{(m)} s_i}(\tau) = \mathrm{R}_{s_i s_i}^{(m)}(\tau), \quad m = 2, 4, \ldots, 2n. \end{aligned} \tag{10}$$

Since $\mathrm{R}_{s_i s_i}^{(m)}(0) = 0, \; m = 1, 2, \ldots, n,$ we obtain $\mathrm{R}_{\bar{\mathbf{s}}}(\tau)$ for $\tau = 0$ by putting (9) and (10) into (8).

$$\mathrm{R}_{\bar{\mathbf{s}}}(0) = \begin{bmatrix} \mathbf{I} & 0 & \ldots & 0 \\ 0 & \mathrm{R}_{\boldsymbol{s}^{(1)}\boldsymbol{s}^{(1)}}(0) & 0 & \vdots \\ \vdots & 0 & \ddots & 0 \\ 0 & \ldots & 0 & \mathrm{R}_{\boldsymbol{s}^{(n)}\boldsymbol{s}^{(n)}}(0) \end{bmatrix}, \tag{11}$$

which means $\mathrm{R}_{\bar{\mathbf{s}}}(0)$ is diagonal. However, note that $\mathrm{R}_{\bar{\mathbf{s}}}(\tau)$ is, in general, not diagonal for nonzero lags. Based on the above analysis, the covariance matrix for the observed signals can be expressed as

$$\begin{aligned} \mathrm{R}_{\mathbf{x}}(\tau) &= [\mathbf{x}(t)\mathbf{x}(t+\tau)^{\mathrm{T}}] \\ &= \mathbf{A}\mathrm{R}_{\bar{\mathbf{s}}}(\tau)\mathbf{A}^{\mathrm{T}} + \sigma_p^2 \delta(\tau)\mathbf{I}. \end{aligned} \tag{12}$$

In the case of $\tau = 0$, we have

$$\mathrm{R}_{\mathbf{x}}(0) = \mathbf{A}\mathrm{R}_{\bar{\mathbf{s}}}(0)\mathbf{A}^{\mathrm{T}} + \sigma_p^2 \mathbf{I}, \tag{13}$$

where σ_p^2 is the noise variance. Because $\mathrm{R}_{\bar{\mathbf{s}}}(0)$ is diagonal, we can use the eigenvalue decomposition of $\mathrm{R}_{\mathbf{x}}(0)$ to estimate both the noise variance and the whitening matrix, **W**, as done in the SOBI approach in [8]. As shown in [6], we can obtain the noise variance by taking the average of $M-(n+1)N$ smallest eigenvalues of $\mathrm{R}_{\mathbf{x}}(0)$.

$$\hat{\sigma}_p^2 = \frac{1}{M-(n+1)N} \sum_{i=(n+1)N+1}^{M} \lambda_i, \tag{14}$$

where λ_i are descending-ordered eigenvalues of $\mathrm{R}_{\mathbf{x}}(0)$. Then, the whitening matrix **W** can be estimated as

$$\mathbf{W} = \begin{bmatrix} (\lambda_1 - \hat{\sigma}_p^2)^{-\frac{1}{2}} h_1 \\ (\lambda_2 - \hat{\sigma}_p^2)^{-\frac{1}{2}} h_2 \\ \vdots \\ (\lambda_{(n+1)N} - \hat{\sigma}_p^2)^{-\frac{1}{2}} h_{(n+1)N} \end{bmatrix}, \tag{15}$$

where h_i are the corresponding eigenvectors of λ_i.

Now we get the whitened observation $\mathbf{y}(t) = \mathbf{W}\mathbf{x}(t)$ and its covariance, which is denoted by

$$\mathrm{R}_{\mathbf{y}}(\tau) = \mathbf{W}\mathbf{A}\mathrm{R}_{\bar{\mathbf{s}}}(\tau)\mathbf{A}^{\mathrm{T}}\mathbf{W}^{\mathrm{T}} + \sigma_p^2 \delta(\tau)\mathbf{I}. \tag{16}$$

2. Rotation

Since the covariance matrix for the observed signals $\mathrm{R}_{\mathbf{x}}(\tau)$ is not diagonal for $\tau \neq 0$, classical rotation, which consists of diagonalization [11] and joint diagonalization [8], cannot be applied to our extended model in (5). In this paper, we use the auto-covariance equalization approach (Rtau Delay) proposed in [6] to recover sources from the whitened observation.

From (10), we know $\mathrm{R}_{s_i s_i^{(m)}}(\tau) + \mathrm{R}_{s_i^{(m)} s_i}(\tau) = 0$ when *m* is odd. However, under our two aforementioned assumptions, sources are mutually uncorrelated so that the covariance matrix $\mathrm{R}_{s_i s_i}(\tau)$ can be approximately seen as constant. Under this approximate assumption, $\mathrm{R}_{s_i s_i^{(m)}}(\tau) + \mathrm{R}_{s_i^{(m)} s_i}(\tau) \approx 0$ when *m* takes an even value. Similar to the Rtau Delay approach in [6], we construct a diagonal matrix by combining $\mathrm{R}_{\bar{\mathbf{s}}}(\tau)$ and its transpose as follows:

$$\frac{\mathrm{R}_{\bar{\mathbf{s}}}(\tau) + \mathrm{R}_{\bar{\mathbf{s}}}(\tau)^{\mathrm{T}}}{2} \approx \begin{bmatrix} \mathrm{R}_{\boldsymbol{ss}}(\tau) & 0 & \ldots & 0 \\ 0 & \mathrm{R}_{\boldsymbol{s}^{(1)}\boldsymbol{s}^{(1)}}(\tau) & \ldots & 0 \\ \vdots & \vdots & \ddots & \vdots \\ 0 & \ldots & 0 & \mathrm{R}_{\boldsymbol{s}^{(n)}\boldsymbol{s}^{(n)}}(\tau) \end{bmatrix}. \tag{17}$$

Then, elaborating from (16), we obtain

$$\frac{\mathrm{R_y}(\tau)+\mathrm{R_y}(\tau)^{\mathrm{T}}}{2} \approx \mathbf{WA}\begin{bmatrix} \mathrm{R}_{ss}(\tau) & 0 & \cdots & 0 \\ 0 & \mathrm{R}_{s^{(1)}s^{(1)}}(\tau) & \cdots & 0 \\ \vdots & \vdots & \ddots & \vdots \\ 0 & \cdots & 0 & \mathrm{R}_{s^{(n)}s^{(n)}}(\tau) \end{bmatrix}\mathbf{A}^{\mathrm{T}}\mathbf{W}^{\mathrm{T}}. \quad (18)$$

Therefore, we can see that **WA** is a unitary matrix [8]–[9] from the whitening. This unitary matrix can be estimated by the joint diagonalization of $\mathrm{R_y}(\tau)+\mathrm{R_y}(\tau)^{\mathrm{T}}$ at multiple nonzero delays from (18).

Finally, after whitening and rotation, we can identify N pairs of original sources and their respective derivatives by cross correlation between reconstructed signals in the extended source vector. Then, for each identified pair, the signal with lower median frequency is identified as the original source.

III. Simulation Results and Analysis

In this section, we choose two ($N = 2$) band-limited Gaussian noise signals with different but overlapping spectra, with zero-mean and unit variance. The sample rate is set at 1,024 Hz and the number of samples is 8,129. For more reliable and reasonable simulation results, we conducted 500 independent Monte Carlo runs for each simulation, in which the mixing matrix is chosen randomly. The maximum bandwidth of the sources is $f_{\max}$ = 350 Hz; and the corresponding delay is t_d = 0.64 ms (according to (3)). The cross-correlation index (CCI) and mean square error (MSE) are chosen as the performance criteria, in which the CCI is the average of the maximal values of the normalized cross-correlation functions between the actual sources and the corresponding algorithm estimations, which is denoted by

$$\mathrm{CCI} = \frac{1}{N}\sum_{i=1}^{N}\max\left\{\left|\mathrm{R}_{s_j\hat{s}_j}\right|\right\}. \quad (19)$$

Because a high-order Taylor approximation creates a computational complexity, we only apply a sixth-order Taylor approximation in this paper — the performance of which is compared with those of SOBI in [8] and Rtau Delay in [6].

1. Simulation 1

In this section, the maximal delays (delays were simulated randomly between 0 and the maximum value T_d) in the mixtures were 0 t_d, 0.3 t_d, 0.6 t_d, 0.9 t_d, 1 t_d, 2 t_d, 3 t_d, 4 t_d, 5 t_d, 6 t_d, 7 t_d, 8 t_d, 9 t_d, and 10 t_d. The time delay of the sources for different mixtures is chosen randomly under the condition $t_{ij} \ll T_d$. In addition, we conducted simulations under the conditions of SNR = ∞ and SNR = 10 dB; the CCI and MSE of which are illustrated in Figs. 1 through 4.

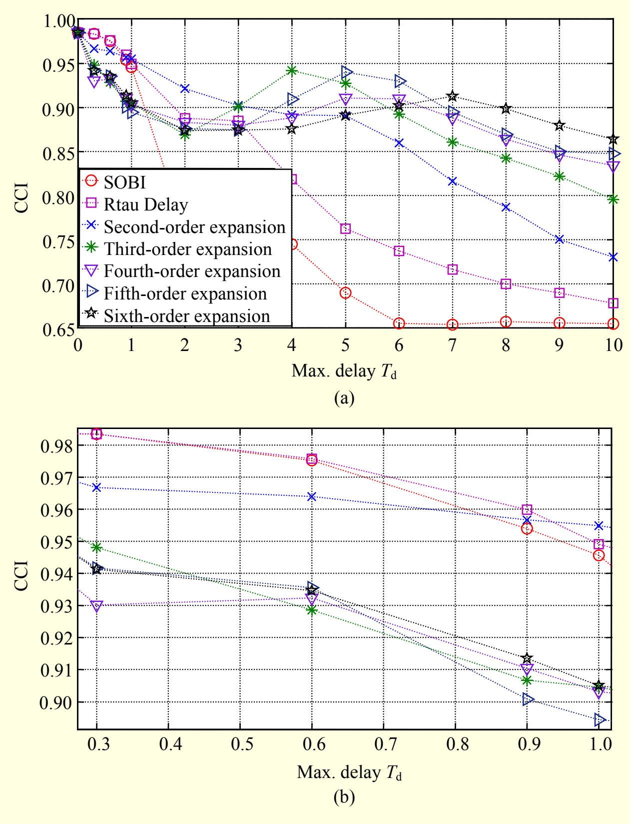

Fig. 1. (a) SNR = ∞, performance index is average maximum value of cross-correlation functions (in %) between two sources and their corresponding estimations averaged over 500 Monte Carlo runs and (b) magnified plot of (a) for maximal delays $T_d = 0\ t_d - 1\ t_d$.

Figures 1 and 2 clearly show that the CCI and MSE values of SOBI and Rtau Delay are slightly larger than those of our proposed high-order approach when the delay is small. This can be seen more clearly in Figs. 1(b) and 2(b), which are magnified plots for maximal delays $T_d = 0\ t_d - 1\ t_d$. For instance, when the delay is 1 t_d, SOBI and Rtau Delay perform better than our method in terms of CCI and MSE.

However, when the delay increases, the advantage of our method becomes more apparent, which can be clearly seen in Figs. 1(a) and 2(a). For example, when the delay is 4 t_d, the CCI of our proposed approach is much larger than in SOBI and Rtau Delay. More precisely, when the delay is 5 t_d, all high-order approximations, from the second-order to the sixth-order, can realize about 90% of the maximum CCI, whereas SOBI can realize about 68%; and Rtau Delay, about 76%. Furthermore, when the delay is larger than 4 t_d, the MSE of our approach is very close to that of SOBI and Rtau Delay. When the delay is 6 t_d, as shown in Fig. 2, our method is slightly better than the other two approaches in terms of MSE.

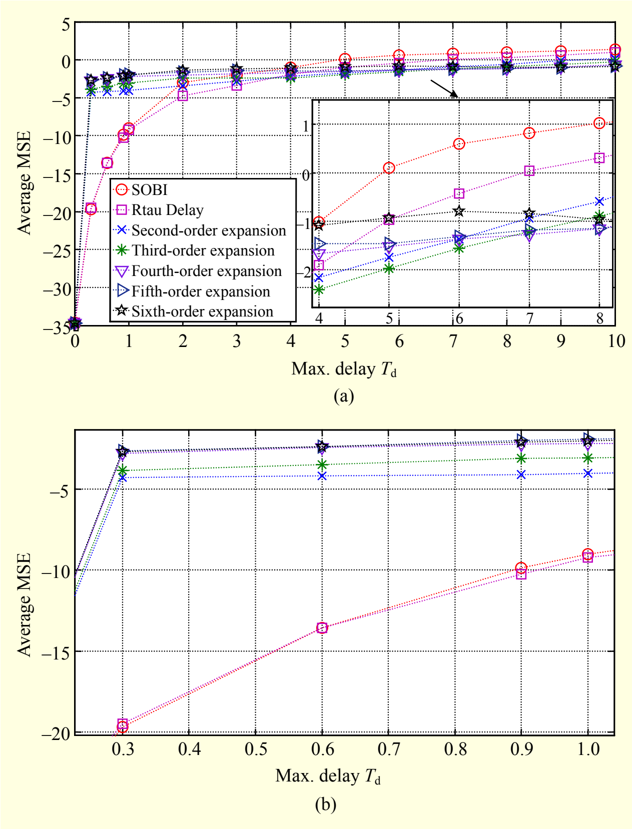

Fig. 2. (a) SNR = ∞, performance index is MSE between two sources and their corresponding estimations averaged over 500 Monte Carlo runs and (b) magnified plot of (a) for maximal delays $T_d = 0\ t_d - 1\ t_d$.

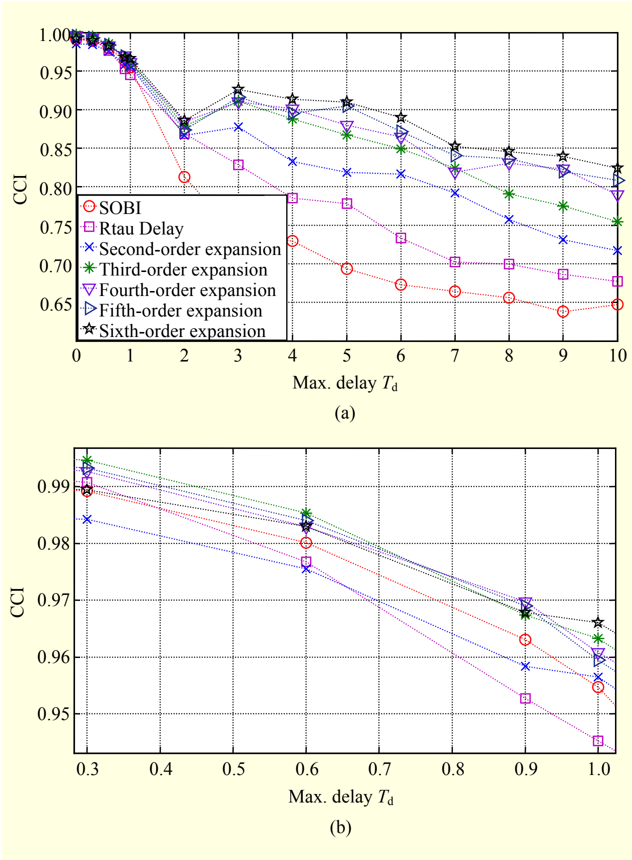

Fig. 3. (a) SNR = 10 dB, performance index is average maximum value of cross-correlation functions (in %) between two sources and their corresponding estimations averaged over 500 Monte Carlo runs and (b) magnified plot of (a) for maximal delays $T_d = 0\ t_d - 1\ t_d$.

As Fig. 1 shows, note that each different nth-order Taylor expansion, under our method, provides a different CCI for a different time delay. When the delay is 2 t_d, the second-order expansion has the best performance, and when the delay is 4 t_d, the third-order expansion performs the best. When the delay varies from 7 t_d to 10 t_d, the sixth-order has the best performance. This phenomenon is caused by the assumption that the correlation between sources becomes weak when the delay is long. In addition, from Fig. 1, we can see that a larger-order approximation outperforms a lower-order expansion when the delay increases, which results from the approximate diagonalization of $\mathrm{R}_x(\tau)$. We will discuss this problem in a future study.

From Figs. 3 and 4, when white Gaussian noise is considered, we can see clearly that the CCI and MSE values of our proposed method are very similar to those of SOBI and Rtau Delay when the delay is small, which can be seen more clearly in Fig. 3(b) and Fig. 4(b), which are magnified plots for the maximum delays $T_d = 0\ t_d - 1\ t_d$. However, when the delay is large, our proposed high-order approximation outperforms the other two approaches, which is shown clearly in Figs. 3(b) and 4(b). More specifically, when the delay varies from 0 t_d to 1 t_d, our method performs very close to that of SOBI and Rtau Delay in terms of CCI and MSE. Conversely, when the delay is more than 2 t_d, our method shows a better CCI and MSE performance than SOBI and Rtau Delay. In addition, it should be noted that the larger the order expansion, the better the performance achieved.

Comparing Figs. 1 through 4, we can conclude that our method is more robust against outside noise. Under a brief delay, our method performs worse than SOBI and Rtau Delay, as shown in Figs. 1 and 2. However, when noise is introduced, our approach performs nearly as well as SOBI and Rtau Delay under a short delay, as shown in Figs. 3 and 4. Moreover, a larger-order expansion shows greater robustness. For instance, a six-order expansion performs the best only when the delay is longer than 7 t_d, as shown in Fig. 1, but it performs the same when the delay is longer than 3 t_d. In other words, our high-order approximation approach is more robust than SOBI and Rtau Delay, and the higher the order, the more robust it is.

It is well accepted that the computational complexity of the

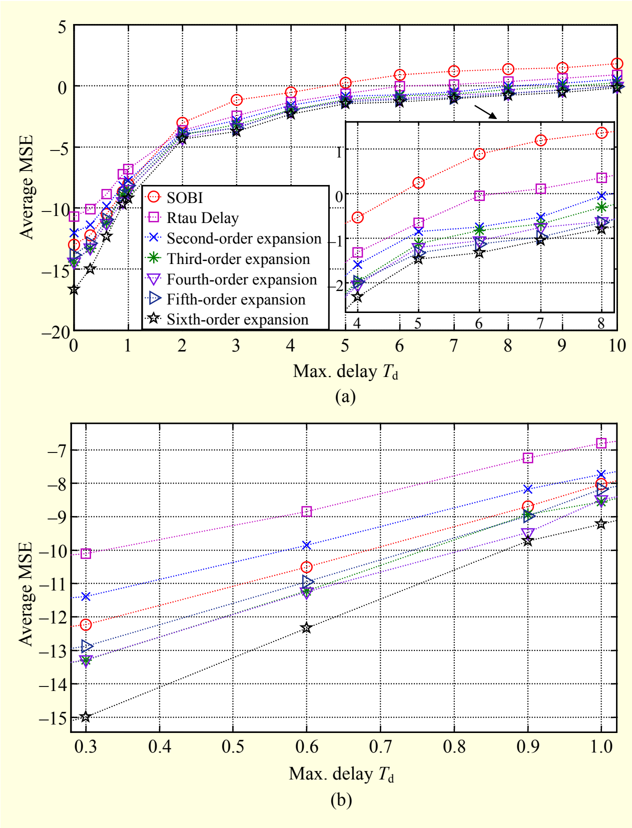

Fig. 4. (a) SNR = 10 dB, performance index is MSE between two sources and their corresponding estimations averaged over 500 Monte Carlo runs, and (b) magnified plot of (a) for maximal delays $T_d = 0\ t_d - 1\ t_d$.

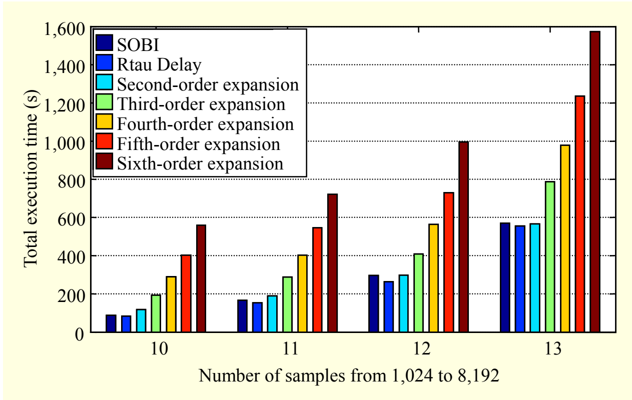

Fig. 5. SNR = ∞; performance index is total execution time for recovering two sources over 500 Monte Carlo runs. In horizontal axes, 10 through 13 denote 2^{10} through 2^{13}, i.e., 1,024 to 8,192.

Taylor series approximation increases enormously when the order is higher. Although a high-order expansion can provide a better performance, especially when noise is present, the computational complexity caused by a high-order Taylor approximation needs to be seriously considered. For this reason, we apply only a sixth-order expansion in this paper. To compare the computational complexity of our method against SOBI and Rtau Delay, we implemented them under the same conditions shown in Figs. 1 and 2 for different numbers of samples from 1,024 to 8,192; the results of which are illustrated in Fig. 5. The execution time was chosen for the measurement criterion, and the computer used is an Intel (R) Core ™ 2 Duo CPU, E8400 @ 3.0 GHz and 2.99 GHz, with 3.00 GB of RAM.

As shown in Fig. 5, we performed 500 independent runs, and the total runtime was recorded for different numbers of samples. The results show that the execution time varies for different approaches and sample sizes. More precisely, when the number of samples is fixed, say at 1,024, the second-order expansion of our method needs approximately the same amount of time as SOBI and Rtau Delay, whereas the time required for the other nth-order expansions increases with an increase in the order. For example, the time for a sixth-order is about six times that of Rtau Delay. When the number of samples increases, the execution time for all methods also increases. When the sample size is 8,192, the time required for SOBI, Rtau Delay, and a second-order is about 580 s, whereas that for the third-order to sixth-order approximations is about 780 s, 980 s, 1,200 s, and 1,580 s, respectively. Actually, it should be noted that the difference between Rtau Delay and the sixth-order is only about 1,000 s. If we average the difference over 500 runs, the difference in time for every run is only around 2 s, which is quite acceptable when the time demand is not very strict. Similarly, the times required for the second-order to fifth-order approximations as compared to that of Rtau Delay are also reasonable. Note that we only apply a sixth-order approximation in this paper, and an expansion higher than the sixth-order is also acceptable and feasible.

2. Simulation 2

From simulation 1, we determined that noise has an influence on the performance of SOBI, Rtau Delay, and our proposed method. To validate the performance of our approach more comprehensively, we conducted simulation experiments by changing the SNR from –10 dB to 15 dB and keeping the delay fixed at either 0.6 t_d or 8 t_d. The results are shown in Figs. 6 through 9.

As shown in Figs. 6 and 7, the advantage of our proposed approach is very apparent over SOBI and Rtau Delay, especially when the SNR is low. When the SNR is lower than 5 dB, the CCI of SOBI and Rtau Delay is about 0.55 and the MSE is more than –2 dB; in this case, the performance is much worse and the sources cannot be successfully recovered. However, under the same conditions, our approach can provide

ETRI Journal, Volume 37, Number 4, August 2015
http://dx.doi.org/10.4218/etrij.15.0114.0527

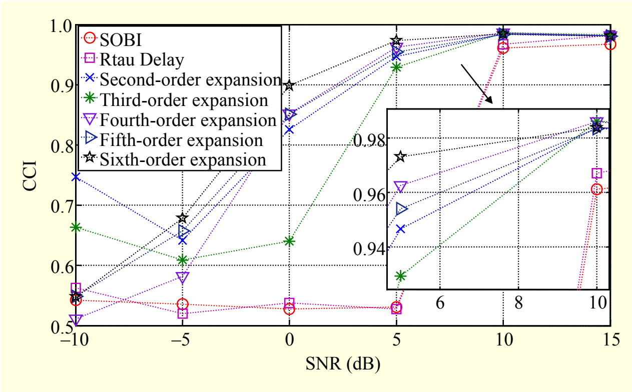

Fig. 6. $T_d = 0.6\ t_d$, SNR = –10 dB to 15 dB; performance index is average maximum value of cross-correlation functions (in %) between two sources and their corresponding estimations averaged over 500 Monte Carlo runs.

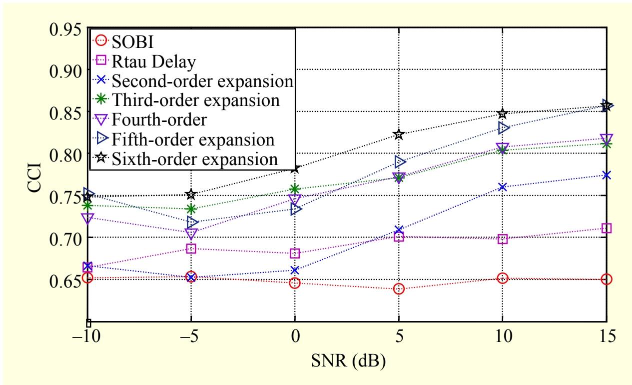

Fig. 8. $T_d = 8\ t_d$, SNR = –10 dB to 15 dB; performance index is average maximum value of cross-correlation functions (in %) between two sources and their corresponding estimations averaged over 500 Monte Carlo runs.

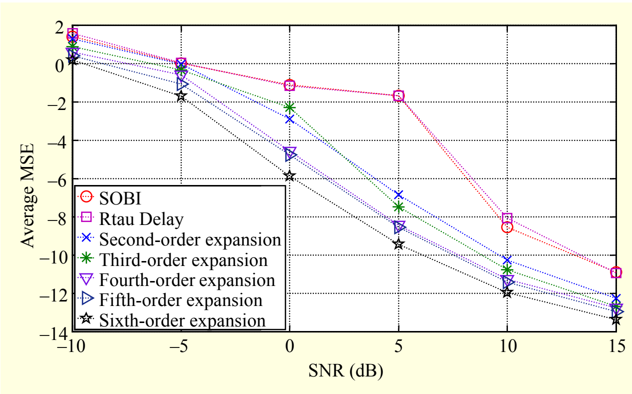

Fig. 7. $T_d = 0.6\ t_d$, SNR = –10 dB to 15 dB; performance index is MSE between two sources and their corresponding estimations averaged over 500 Monte Carlo runs.

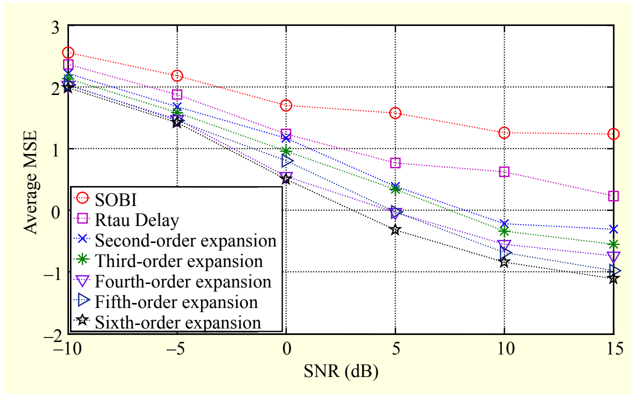

Fig. 9. $T_d = 8\ t_d$, SNR = –10 dB to 15 dB; performance index is MSE between two sources and their corresponding estimations averaged over 500 Monte Carlo runs

a much better performance. For instance, when the SNR = 0 dB, the CCI of the sixth-order is about 0.9 and the MSE is about –6 dB. Thus, our proposed high-order expansion outperforms both SOBI and Rtau Delay at a low SNR, despite the short delay.

When the delay is large, we can see from Figs. 8 and 9 that the CCI and MSE of our method are better than those of SOBI and Rtau Delay with a change in SNR. More precisely, the CCI of SOBI and Rtau Delay at –10 dB is about 0.65 and 0.66, respectively, and about 0.65 and 0.71 at 15 dB. Similarly, their MSE does not change significantly. Conversely, the CCI of the third-order approximation of our method reaches about 0.75 at –10 dB, whereas that of the sixth-order approximation reaches about 0.85 at 15 dB. This is also true for the MSE of our approach; that is, a higher-order approximation with an increase in the SNR provides a better performance than SOBI and Rtau Delay.

Finally, compared with simulations 1 and 2, we can draw the conclusion that a high-order Taylor series expansion approach is more robust than SOBI and Rtau Delay, especially when the SNR is low. In other words, the advantage of our proposed method over SOBI and Rtau Delay under a lengthy delay is extended to a short delay when noise is present.

IV. Conclusion

In this paper, we proposed an extension of a first-order Taylor approximation to a higher order to solve the blind separation of delayed sources based on the SOBI approach. We assume that the correlation between sources becomes weak when the delay is long. Simulation results show that our proposed method outperforms other corresponding approaches under a lengthy delay, and is more robust against noise, particularly when the SNR is low. However, the computational complexity caused by a high-order Taylor expansion should be considered. Future work includes a reduction of the computational complexity of a high-order expansion and the extension of our method to a convolution mixture model.

References

[1] H.F. Zhang, L.P. Li, and W.C. Li, "Independent Vector Analysis for Convolutive Blind Noncircular Source Separation," *Signal Process*., vol. 92, no. 9, Sept. 2012, pp. 2275–2283.

[2] J. Gao, X. Zhu, and A.K. Nandi, "Independent Component Analysis for Multiple-input Multiple-output Wireless Communication Systems," *Signal Process*., vol. 91, no. 4, Apr. 2011, pp. 607–623.

[3] E. Florian, A. Chevreuil, and P.H. Loubaton, "Blind Source Separation of Convolutive Mixtures of Non-circular Linearly Modulated Signals with Unknown Baud Rates," *Signal Process*., vol. 92, no. 3, Mar. 2012, pp. 715–726.

[4] G. Chabriel and J. Barrere, "Blind Identification of Slightly Delayed Mixtures," *IEEE Workshop Statistical Signal Array Process*., Pocono Manor, PA, USA, Aug. 2000, pp. 319–323.

[5] J. Ashtar et al., "A Novel Approach to Blind Separation of Delayed Sources in Linear Mixture," *Semester Signal Process*., Aalborg, Denmark, 2004, pp. 1–8.

[6] N. Jiang and D. Farina, "Covariance and Time-Scale Methods for Blind Separation of Delayed Sources," *IEEE Trans. Biomed. Eng*., vol. 58, no. 3, 2011, pp. 550–556.

[7] L. Omlor and M.S. Giese, "Blind Source Separation for Over-Determined Delayed Mixtures," *Adv. Neural Inf. Process. Syst*., Vancouver, Canada, Dec. 2006, pp. 1049–1056.

[8] A. Belouchrani et al., "A Blind Source Separation Technique Using Second-Order Statistics," *IEEE Trans. Signal Process*., vol. 45, no. 2, Feb. 1997, pp. 434–444.

[9] D. Farina, M.F. Lucas, and C. Doncarli, "Optimized Wavelets for Blind Separation of Non-stationary Surface Myoelectric Signals," *IEEE Trans. Biomed. Eng*., vol. 55, no. 1, Jan. 2008, pp. 78–86.

[10] K.S. Shanmugan and A.M. Breipohl, "*Random Signals: Detection, Estimation, and Data Analysis*," New York, NY, USA: Wiley, 1988, pp. 25–32.

[11] L. Tong et al., "Indeterminacy and Identifiability of Blind Identification," *IEEE Trans. Circuits Syst*., vol. 38, no. 5, May 1991, pp. 499–509.

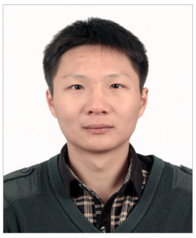

Wei Zhao received his BS degree in electrical and information engineering from Nanjing University of Information Science and Technology, China, in 2011. He is currently pursuing his PhD degree in information and communication engineering, PLA University of Science and Technology, Nanjing, China. His research interests include blind source separation, independent component analysis, compressed sensing, sparse component analysis, and their corresponding applications in wireless communication systems.

Zhigang Yuan received his PhD degree in information and communication engineering, in 2008, from PLA University of Science and Technology (PLAUST), Nanjing, China. Since 2008, he has been with the College of Communications Engineering of PLAUST, where he is a lecturer. His research interests include digital transmission technology and digital communication signal processing.

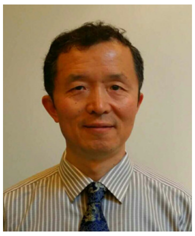

Yuehong Shen received his PhD degree in communication and information systems, in 1999, from Nanjing University of Science and Technology, China. Since 1999, he has been with the College of Communications Engineering of PLA University of Science and Technology, Nanjing, China, where he is a professor. His research interests include wireless MIMO communication, digital signal processing, statistical signal analysis, and wireless statistic division multiplexing.

Yufan Cao received his BS degree in electrical and circuit systems, in 2013, from PLA University of Science and Technology (PLAUST), Nanjing, China. He is currently pursuing his MS degree in information and communication engineering, PLAUST. His research interests include blind source separation, independent component analysis, and their corresponding applications in wireless communication systems.

http://dx.doi.org/10.4218/etrij.15.0114.0527

Yimin Wei received his PhD degree in communication and information systems, in 2012, from PLA University of Science and Technology (PLAUST), Nanjing, China. Since 2003, he has been with the College of Communications Engineering of PLAUST, where he is an assistant professor. His research interests include wireless communication and signal processing.

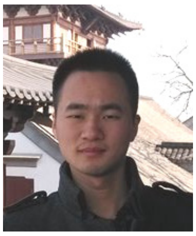

Pengcheng Xu received his BS degree in electrical and information engineering from Anhui University, Hefei, China, in 2009. He is currently pursuing his PhD degree in information and communication engineering at PLA University of Science and Technology, Nanjing, China. His research interests include blind source separation, independent component analysis, and their corresponding applications in wireless communication systems.

Wei Jian received his PhD degree in information and communication engineering, in 2006, from PLA University of Science and Technology (PLAUST), Nanjing, China. Since 2006, he has been with the College of Communications Engineering of PLAUST, where he is a lecturer. His research interests include digital transmission technology and wireless communication signal processing.